



Published in final edited form as:

Addict Neurosci. 2023 December 15; 9: . doi:10.1016/j.addicn.2023.100137.

Prefrontal cortex glutamatergic adaptations in a mouse model of alcohol use disorder

Mahum T. Siddiqi^a, Dhruba Podder^a, Amanda R. Pahng^{b,c}, Alexandria C. Athanason^a, Tali Nadav^d, Chelsea Cates-Gatto^d, Max Kreifeldt^e, Candice Contet^e, Amanda J. Roberts^d, Scott Edwards^b, Marisa Roberto^e, Florence P. Varodayan^{a,e,*}

^aDevelopmental Exposure Alcohol Research Center and Behavioral Neuroscience Program, Department of Psychology, Binghamton University-SUNY, 4400 Vestal Parkway East, Binghamton, NY, 13902, USA

^bDepartment of Physiology, Louisiana State University Health Sciences Center, 533 Bolivar Street, New Orleans, LA, 70112, USA

^cSoutheast Louisiana Veterans Health Care System, 2400 Canal Street, 11F, New Orleans, LA, 70119, USA

^dAnimal Models Core Facility, The Scripps Research Institute, 10550 North Torrey Pines Road, La Jolla, CA, 92037, USA

^eDepartment of Molecular Medicine, The Scripps Research Institute, 10550 North Torrey Pines Road, La Jolla, CA, 92037, USA

Abstract

Alcohol use disorder (AUD) produces cognitive deficits, indicating a shift in prefrontal cortex (PFC) function. PFC glutamate neurotransmission is mostly mediated by α -amino-3-hydroxy-5-methyl-4-isoxazolepropionic acid-type ionotropic receptors (AMPA); however preclinical studies have mostly focused on other receptor subtypes. Here we examined the impact of early withdrawal from chronic ethanol on AMPAR function in the mouse medial PFC (mPFC).

This is an open access article under the CC BY-NC-ND license (<http://creativecommons.org/licenses/by-nc-nd/4.0/>).

*Corresponding author at: Department of Psychology, Binghamton University-SUNY, S4-175G, 4400 Vestal Parkway East, Binghamton, NY 13902, USA. fvaroday@binghamton.edu (F.P. Varodayan).

CRediT authorship contribution statement

Mahum T. Siddiqi: Formal analysis, Investigation, Visualization, Writing – original draft, Writing – review & editing. **Dhruba Podder:** Formal analysis, Investigation. **Amanda R. Pahng:** Formal analysis, Investigation, Methodology, Validation, Visualization, Writing – review & editing. **Alexandria C. Athanason:** Formal analysis, Investigation, Writing – review & editing. **Tali Nadav:** Formal analysis, Investigation. **Chelsea Cates-Gatto:** Formal analysis, Investigation. **Max Kreifeldt:** Investigation. **Candice Contet:** Funding acquisition, Methodology, Resources, Supervision, Writing – review & editing. **Amanda J. Roberts:** Funding acquisition, Methodology, Resources, Supervision, Writing – review & editing. **Scott Edwards:** Funding acquisition, Methodology, Resources, Supervision, Writing – review & editing. **Marisa Roberto:** Funding acquisition, Resources, Supervision, Writing – review & editing. **Florence P. Varodayan:** Conceptualization, Formal analysis, Funding acquisition, Investigation, Methodology, Resources, Supervision, Validation, Visualization, Writing – original draft, Writing – review & editing.

Declaration of Competing Interest

The authors declare that they have no known competing financial interests or personal relationships that could have appeared to influence the work reported in this paper.

Supplementary materials

Supplementary material associated with this article can be found, in the online version, at doi:10.1016/j.addicn.2023.100137.

Dependent male C57BL/6J mice were generated using the chronic intermittent ethanol vapor-two bottle choice (CIE-2BC) paradigm. Non-dependent mice had access to water and ethanol bottles but did not receive ethanol vapor. Naïve mice had no ethanol exposure. We used patch-clamp electrophysiology to measure glutamate neurotransmission in layer 2/3 prelimbic mPFC pyramidal neurons. Since AMPAR function can be impacted by subunit composition or plasticity-related proteins, we probed their mPFC expression levels. Dependent mice had higher spontaneous excitatory postsynaptic current (sEPSC) amplitude and kinetics compared to the Naïve/Non-dependent mice. These effects were seen during intoxication and after 3–8 days withdrawal, and were action potential-independent, suggesting direct enhancement of AMPAR function. Surprisingly, 3 days withdrawal decreased expression of genes encoding AMPAR subunits (*Gria1/2*) and synaptic plasticity proteins (*Dlg4* and *Grip1*) in Dependent mice. Further analysis within the Dependent group revealed a negative correlation between *Gria1* mRNA levels and ethanol intake. Collectively, these data establish a role for mPFC AMPAR adaptations in the glutamatergic dysfunction associated with ethanol dependence. Future studies on the underlying AMPAR plasticity mechanisms that promote alcohol reinforcement, seeking, drinking and relapse behavior may help identify new targets for AUD treatment.

Keywords

Addiction; AMPA; GluR1; Neuroplasticity; Excitatory transmission

Introduction

Alcohol use disorder (AUD) is a chronic, relapsing disease characterized by repeated bouts of heavy drinking interspersed with abstinence periods. These cycles of intoxication/withdrawal produce long-lasting changes in brain structure and function that promote further alcohol (ethanol) consumption and disease progression. The prefrontal cortex (PFC) is particularly vulnerable to alcohol, with *postmortem* studies on PFC tissue from individuals with AUD revealing reduced volume, altered neuronal morphology, and cellular and synaptic loss [1]. These neuroadaptations are accompanied by altered PFC activity in networks related to executive control and reward processing, and are thought to underlie the deficits in attention, inhibitory control, working memory and cognitive flexibility that persist into abstinence [1,2].

Glutamate is the most abundant excitatory neurotransmitter in the brain, and individuals with AUD often experience glutamatergic dysfunction [3–5]. Alterations in glutamatergic signaling can vary depending on regions studied, AUD severity, amount of alcohol consumed, length of abstinence period, etc., with some studies reporting elevations in PFC glutamate in individuals with AUD [6–8], while others found reductions [9,10]. Despite the dynamic nature of alcohol-induced glutamate dysfunction, PFC glutamate levels have been correlated with alcohol craving, loss of control over alcohol intake, cognitive deficits and AUD severity [6,7,9–11]. Rodents exposed to chronic ethanol exhibit similar indices of medial PFC (mPFC) glutamatergic dysfunction, including neuronal activation, dendritic remodeling, spine maturation and increased glutamatergic signaling, though the underlying mechanisms are less well described [8,12–23].

Most mechanistic work on ethanol's glutamatergic effects has focused on *N*-methyl-d-aspartate receptors (NMDARs), as they are considered the glutamate receptor subtype most sensitive to ethanol [3,24,25]. However, NMDAR function often requires activation of α -amino-3-hydroxy-5-methyl-4-isoxazolepiopionic acid-type ionotropic glutamate receptors (AMPA receptors), and the two types of receptors work together to mediate different forms of synaptic plasticity including long-term potentiation (LTP) [3,26]. Accordingly, there have been a limited number of human and preclinical studies that have found alcohol-induced changes in PFC/mPFC AMPAR binding and expression [12,27–32]. Additionally, we reported previously that withdrawal from chronic ethanol increases AMPAR function and dendritic spine maturity specifically in layer 2/3 pyramidal neurons in the prelimbic mPFC, the latter of which could potentially increase the density of AMPAR anchoring in the postsynaptic terminal [33]. AMPARs are heterotetrameric protein complexes composed of four core subunits (GluA1–4), auxiliary subunits and interacting proteins [26], and their specific composition dictates their trafficking and function to modulate synaptic strength. Therefore, there is a need for more direct investigation of the chronic ethanol-induced molecular changes that underlie mPFC glutamatergic plasticity.

Here we examined the impact of 3–8 days withdrawal from chronic ethanol exposure on the mouse mPFC using the chronic intermittent ethanol vapor-two bottle choice (CIE-2BC) model. Prelimbic mPFC AMPAR-mediated neurotransmission and mPFC transcript levels of the most common AMPAR subunits expressed in the adult brain (GluA1–3; [26]) were measured. We also investigated mPFC GluA1 protein levels, as well as GluA1 phosphorylation sites related to plasticity [34,35]. Finally, mPFC gene expression of synaptic scaffolding proteins (postsynaptic density 95, PSD95 encoded by the *Dlg4* gene, and glutamate receptor-interacting protein encoded by the *Grip1* gene) were examined. Thus, here we used molecular and cellular physiology approaches in a mouse model of chronic ethanol exposure to investigate the molecular changes that underlie mPFC glutamatergic plasticity.

Materials & methods

Study design

Adult male C57BL/6J mice ($n = 98$; 30.1 ± 0.3 g) were purchased from The Jackson Laboratory (Bar Harbor; ME). Biological males were designated based on external anatomy prior to shipping and visually confirmed on site. 3–4 mice were housed per cage with ad libitum food and water, with cages maintained in a temperature- and humidity-controlled vivarium on a reverse 12 h light/dark cycle. All procedures comply with the ARRIVE guidelines and were approved by The Scripps Research Institute (TSRI) Institutional Animal Care and Use Committee, consistent with the National Institutes of Health Guide for the Care and Use of Laboratory Animals. Experimental sample sizes were determined using power analyses based on prior studies.

Chronic intermittent ethanol-two bottle choice model

The CIE-2BC model was used to generate three groups of mice: 1) Naïve mice that only drank water, 2) Non-dependent mice (Non-dep) that had access to water and ethanol bottles,

and Dependent mice (Dep) that were exposed to CIE vapor which then led to an escalation of their ethanol drinking (Fig. 1A and B). CIE consistently produces ethanol dependence in mice, as reflected by increased ethanol drinking behavior, anxiety-like behavior, reward deficits and sleep disruptions [33,36–40]. To establish baseline 2BC drinking, for 5 days per week for 2–4 weeks, mice were transferred to individual fresh cages 30 min prior to lights off and given 2-h access to two drinking tubes (15% w/v ethanol and tap water). Mice were returned to their group-housed home cages after each drinking session. Naïve mice ($N=36$) received 2 water bottles. Total ethanol consumption during the last week of baseline drinking was used to evenly assign each cage of mice to the Non-dependent ($N=22$) or Dependent ($N=40$) group (Week 1 on Fig. 1C and D). This assignment is based on cages since the mice are group-housed during vapor exposure. To generate the Dependent group, we used a 2-week protocol that consisted of 4 days of CIE (16 h per day in ethanol vapor followed by 8 h of withdrawal using air exposure in chambers from La Jolla Alcohol Research (La Jolla, CA), 3 days of forced abstinence, 5 days of 2BC drinking (same parameters as in baseline training), and 2 days of forced abstinence. Mice received an *i.p.* injection of 1.75 g/kg ethanol + 68.1 mg/kg of the alcohol dehydrogenase inhibitor pyrazole (Sigma, St Louis, MO) before each vapor exposure. This 2-week protocol was repeated for 5–6 cycles. Tail blood samples were collected immediately after removal from the vapor chambers into heparinized capillary tubes and centrifuged for 20 min at 13,000 rpm at 4 °C. The supernatants were then processed on an Agilent 7820A gas chromatograph coupled to a 7697A headspace sampler with targeted blood ethanol levels (BEL) that reliably produce dependence (150–250 mg/dL). Non-dep mice underwent a similar protocol, with weeks of pyrazole (in saline) injections/air exposure interspersed with weeks of 2BC drinking [36,37,39–43]. Naïve mice also received pyrazole (in saline) injections, but their 2BC sessions used 2 water bottles. It is important to note that the Non-dependent group was designed to be used as a secondary control to determine whether changes observed in Dependent mice specifically result from the CIE (which produces the dependent phenotype) or from ethanol drinking alone. Due to the differences in brain tissue preparation required for each study, separate cohorts that were sequentially run were used for: 1) the electrophysiological recordings (some mice euthanized immediately after their last ethanol vapor session and some mice euthanized after 3–8 full days of withdrawal with the data from each timepoint presented separately; mean BEL achieved during ethanol vapor exposure was 150.6 ± 12.1 mg/dL), 2) gene expression analyses (mice euthanized after 3 days of withdrawal; mean BEL was 214.0 ± 18.43 mg/dL), and 3) protein expression analyses (mice euthanized immediately after their last ethanol vapor session; mean BEL was 158.6 ± 7.9 mg/dL).

Glutamatergic transmission

Ex vivo patch-clamp electrophysiology recordings were conducted as previously described [33,39,40]. Mice ($N=11$ –18 mice per group) were anesthetized using 3–5 % isoflurane either immediately (Supplementary Fig. 1) or 3–8 full days after CIE vapor (Figs. 2 and 3). Brains were placed in ice-cold, oxygenated high sucrose solution (pH 7.3–7.4): 206 mM sucrose; 2.5 mM KCl; 0.5 mM CaCl_2 ; 7 mM MgCl_2 ; 1.2 mM NaH_2PO_4 ; 26 mM NaHCO_3 ; 5 mM glucose; 5 mM HEPES, and 300 μm coronal brain slices were sectioned (Leica VT1200 S; Buffalo Grove, IL). Slices were incubated in oxygenated artificial cerebrospinal

fluid (aCSF): 130 mM NaCl, 3.5 mM KCl, 2 mM CaCl₂, 1.25 mM NaH₂PO₄, 1.5 mM MgSO₄, 24 mM NaHCO₃, and 10 mM glucose for 30 min at 32 °C and then for a minimum of 30 min at room temperature. Prelimbic layer 2/3 pyramidal neurons were located 100–300 μm from the pial surface and identified by their characteristic size and shape using infrared-differential interference contrast (IR-DIC) optics, a w60 water immersion objective (Olympus BX51WI) and a CCD camera (EXi Aqua, QImaging), [33,39,40,44]. Whole-cell voltage-clamp recordings from 88 neurons were collected in gap-free acquisition mode with a 20 kHz sampling rate and 10 kHz low-pass filter using a Multiclamp 700B amplifier, Digidata 1440A and pClamp 10.2 software (all Molecular Devices, Sunnyvale, CA). 5–7 MΩ pipettes were filled with internal solution: 145 mM K-gluconate, 5 mM EGTA, 2 mM MgCl₂ 10 mM HEPES, 2 mM Mg⁺⁺-ATP, 0.2 mM Na⁺-GTP. Cells were held at –70 mV and spontaneous excitatory postsynaptic currents (sEPSCs) were collected in the presence of the GABA receptor antagonists 1 μM CGP 55845A (Tocris Biosciences, Ellisville, MI) and 30 μM bicuculline (Sigma, St. Louis, MO). 0.5 μM tetrodotoxin (Sigma) was also added to the bath solution to record action potential-independent miniature EPSCs (mEPSCs). We have previously shown that these s/mEPSCs are primarily mediated by AMPARs [33]. s/mEPSC recordings with a series resistance >15 MΩ or a >20 % change in series resistance, as monitored with a 10 mV pulse, were excluded. Data for each treatment group were collected from 1 to 3 cells per animal from a minimum of 5 mice. s/mEPSC analysis of frequency, amplitude, rise time and decay time was performed blind to the animal treatment group using Mini Analysis (Synaptosoft Inc., Fort Lee, NJ). Events <5 pA, and cells with <60 events in a 3 min interval were excluded. In these experiments, higher frequencies indicate greater neurotransmitter release probabilities, while higher amplitude and kinetics reflect enhanced postsynaptic receptor function [45].

Glutamatergic receptor and plasticity gene expression

Real time polymerase chain reaction (rt-PCR) analyses were conducted as previously described [36]. Mice ($N = 10–12$ per group) were anesthetized with 3–5 % isoflurane 3 full days after CIE vapor. Brains were extracted, flash frozen, stored at –80 °C, and then shipped from The Scripps Research Institute to Binghamton University. Midline micropunches (0.75 mm) enriched for the mPFC were collected, and homogenized in Trizol reagent (Sigma-Aldrich, St. Louis, MO) with 5 mm stainless steel beads (Qiagen, Hilden, Germany) and a TissueLyser (Qiagen, Valencia, CA). Total RNA was extracted using RNeasy columns (Qiagen), with the concentration and purity measured using a Nanodrop spectrophotometer (ThermoScientific, Waltham, MA). The QuantiTect Reverse Transcription kit (Cat. No. 205,313, Qiagen) was used to make cDNA, which was stored at –20 °C. rt-PCR was performed using the CFX384 real-time PCR detection system, IQ SYBER Green Supermix (Biorad, Hercules, CA), and cDNA template and gene primers (Table 1). A single peak in the melt curve was used to confirm the specificity of each primer pair for the target genes. TATA-box binding protein (*Tbp*; Supplementary Fig. 2A) was used as a reference gene to normalize gene expression data using the C_q method. The percent change from control was then calculated with the Naïve group selected as the ultimate control. All final data points falling in the outlier range of ± 2 standard deviations were excluded.

Glutamatergic receptor protein expression

Western blot analyses were conducted as previously described [40,46]. Mice ($N=12$ per group) were anesthetized with 3–5 % isoflurane immediately after their last CIE vapor and decapitated. After mouse brains were removed rapidly, they were snap-frozen in isopentane, stored fresh-frozen at -80°C and then shipped from The Scripps Research Institute to Louisiana State University Health Sciences Center. Brains were moved from -80°C storage to -20°C 24 h prior to brain region dissection. During dissection on the cryostat (-12°C), mPFC brain punches (0.5 mm thick, 16-gage needle) were taken from frozen and mounted brain tissue according to [47]. Brain punches were stored at -80°C until they were homogenized by sonication in a lysis buffer (320 mM sucrose, 5 mM HEPES, 1 mM EGTA, 1 mM EDTA, 1 % SDS), phosphatase inhibitor cocktails II and III (diluted 1:100), and protease inhibitor cocktail (diluted 1:100; Sigma, St. Louis, MO, USA). mPFC tissue homogenates were heated (95°C for 5 min) and total protein concentrations were measured using a detergent-compatible Lowry method (Bio-Rad, Hercules, CA, USA). Samples were aliquoted and stored (-80°C). Protein samples (20 μg) were electrophoretically separated by SDS-polyacrylamide gel using a Tris/Tricine/SDS buffer system (Bio-Rad) and transferred to polyvinylidene difluoride membranes (GE Healthcare, Piscataway, NJ, USA). After blocking membranes in 5 % non-fat milk at room temperature for 1 h, membranes were incubated in 2.5 % non-fat milk with primary antibody at 4°C overnight. The primary antibodies were phospho-GluA1-Ser831 (1:1000; Cell Signaling; Cat # 75,574) and phospho-GluA1-Ser845 (1:2000; Cell Signaling; Cat # 8084). Membranes were washed and incubated (1 h at room temperature) with species-specific peroxidase-conjugated secondary antibody (1:10,000; Bio-Rad). After the final wash, membranes were incubated in a chemiluminescent reagent (Immobilon Crescendo Western HRP Substrate, Millipore Corporation, Billerica, MA, USA). After exposing membranes to film for development, they were stripped for 30 min at room temperature (Restore; Thermo Scientific) and reprobbed for total GluA1 (1:2000; Cell Signaling; Cat # 13,185) and β -tubulin (1:1000,000; Santa Cruz Biotechnology; Cat # sc-53,140) levels. Densitometry was used to detect band immunoreactivity (Image J 1.45S; Bethesda, MD, USA) and values were expressed as a percentage of the mean of the Naïve controls for each gel to normalize the data across the blots (full blots in Supplementary Figs. 3–6). As a loading control, there was no group difference in β -tubulin between the Naïve and Dependent mice (Supplementary Fig. 2B). Finally, the percent change from control was calculated with the Naïve group selected as the ultimate control. All final data points falling in the outlier range of ± 2 standard deviations were excluded.

Statistics

Statistical analyses were performed using one-sample and unpaired t -tests, Pearson correlations, and one-way ANOVAs with *post hoc* Tukey's multiple comparisons tests where appropriate, with differences significant at $p < 0.05$ (Prism v9, GraphPad, San Diego, CA). Data are represented as mean \pm SEM.

Results

Ethanol intake escalated in dependent mice

As expected, CIE vapor exposure caused the majority of Dependent mice to escalate their ethanol intake between the last week of baseline 2BC drinking (Week 1) and the final week of 2BC drinking (Week 6; 35 out of 40 mice), while only 13 out of 22 Non-dependent mice did so (Fig. 1A–D). Similar to our previous work [36,39,40], Dependent mice had a higher ethanol intake in their final week of 2BC drinking (Week 6) and when totaled across all 2BC drinking sessions compared to Non-dependent mice (Week 6: $t(60) = 3.93$, $p < 0.001$; total: $t(60) = 2.85$, $p < 0.01$ by unpaired t -test; Fig. 1E and F).

Enhanced prelimbic mPFC glutamate receptor function in dependent mice

We first examined the impact of 3–8 days ethanol withdrawal on glutamate transmission in prelimbic mPFC layer 2/3 pyramidal neurons. There were no differences in sEPSC frequencies across all three groups (frequency: $F(2, 42) = 0.76$, $p = 0.47$ by one-way ANOVA; Fig. 2A–C). However, Dependent mice had significantly higher sEPSC amplitudes, rise times and decay times compared to Naïve and Non-dependent mice (amplitude: $F(2, 42) = 9.23$, $p < 0.001$; rise time: $F(2, 42) = 17.34$, $p < 0.001$; decay time: $F(2, 42) = 14.08$, $p < 0.001$; Fig. 2D–F). In a subset of mice from the Naïve and Dependent groups, we still observed these signs of enhanced glutamate receptor function after tetrodotoxin was added to the bath to block action potentials (mEPSC; frequency: $t(16) = 0.040$, $p = 0.97$; amplitude: $t(16) = 2.61$, $p < 0.05$; rise time: $t(16) = 2.85$, $p < 0.05$; decay time: $t(16) = 1.95$, $p = 0.0692$ by unpaired t -test; Fig. 3). Finally, to probe whether these synaptic changes resulted from the chronic ethanol vapor exposure or the withdrawal period, we performed similar sEPSC recordings on Naïve and Dependent mice euthanized immediately after the last CIE vapor session. There were similar increases in sEPSC amplitude and kinetics in Dependent mice at this intoxication time point (sEPSC frequency: $t(23) = 0.68$, $p = 0.51$; amplitude: $t(23) = 3.21$, $p < 0.01$; rise time: $t(23) = 3.67$, $p < 0.01$; decay time: $t(23) = 3.11$, $p < 0.01$ by unpaired t -test; Supplementary Fig. 1) as we observed previously with 3–8 days withdrawal (see Fig. 2). Since we have previously shown that s/mEPSCs recorded under our electrophysiological conditions are primarily AMPAR-mediated currents [33], collectively, these data suggest that withdrawal after chronic ethanol exposure directly impacts synapses of layer 2/3 pyramidal neurons in the prelimbic mPFC to enhance postsynaptic AMPAR function.

Ethanol dependence decreased glutamate receptor gene and protein levels

We next used rt-PCR to probe the effects of 3 days of withdrawal on mPFC gene expression of GluA1-3 subunits of the AMPAR. There was a significant decrease in *Gria1* and *Gria2* transcript levels in the mPFC of Dependent mice compared to Naïve and Non-dependent mice, with no differences in *Gria3* mRNA (Fig 4; see Table 2 for statistical analyses). Further analyses revealed a negative correlation between *Gria1* gene expression and total ethanol intake within the Dependent group, highlighting a possible link between the two (Fig 4D).

To further assess chronic ethanol-induced changes in GluA1 at the protein level and to begin to probe whether the AMPAR-related plasticity changes we observed after 3 days withdrawal may stem from the chronic ethanol exposure itself or specifically from the withdrawal period, we performed western blotting on mPFC tissue from mice euthanized immediately after CIE vapor (same time point as electrophysiology recordings in Supplementary Fig. 1). Our western blot data revealed a similar reduction in GluA1 protein expression in the mPFC of Dependent mice compared to Naïve mice, though its Ser831 and Ser845 phosphorylation ratios were stable (GluA1: $t(22) = 2.56, p < 0.05$; GluA1-Ser831: $t(22) = 0.52, p = 0.61$; GluA1-Ser845: $t(22) = 0.99, p = 0.33$ by unpaired t -test; Fig. 5).

Ethanol withdrawal decreased plasticity gene expression in dependent mice

Finally, we investigated whether 3 days of withdrawal altered glutamatergic plasticity gene expression in the mPFC. We found that Dependent mice had lower *Grip1* and *Dlg4* mRNA levels compared to the Naïve and Non-dependent groups (Fig. 6A and B; see Table 2 for statistical analyses), but there were no correlations between gene expression and total ethanol intake within the Dependent group (Fig. 6C and D).

Discussion

These data highlight a role for mPFC AMPAR plasticity in the glutamatergic dysfunction associated with ethanol withdrawal. Specifically, Dependent mice had a higher sEPSC amplitude (peak current) and longer sEPSC kinetics (channel activation and desensitization/deactivation times) in layer 2/3 prelimbic mPFC pyramidal neurons compared to Naïve/Non-dependent mice. These postsynaptic effects were also present in intoxicated Dependent mice and were action potential-independent, suggesting that the chronic vapor ethanol directly enhanced AMPAR function. Surprisingly, dependence decreased mPFC GluA1 protein levels during intoxication and decreased mPFC expression of *Gria1* and *Gria2* after 3 full days of withdrawal, indicating that the chronic ethanol exposure itself can generate AMPAR plasticity. Further analyses revealed a negative correlation between *Gria1* mRNA levels and total ethanol intake within the Dependent group, highlighting a possible link between the two. Finally, mPFC mRNA levels of scaffolding proteins that regulate synaptic plasticity (*Dlg4* and *Grip1*) were reduced in early withdrawal.

The most parsimonious explanations for the discrepancies between our functional and molecular data are that separate mice cohorts with different mean BELs achieved during ethanol vapor exposure (electrophysiology: 150.6 ± 12.1 mg/dL; gene expression: 214.0 ± 18.43 mg/dL; protein expression: 158.6 ± 7.9 mg/dL), different mPFC tissue samples (electrophysiology: prelimbic mPFC layer 2/3 pyramidal neurons; gene and protein expression: mPFC tissue punches), and different euthanasia time points (electrophysiology: intoxicated and 3–8 full days of withdrawal; gene expression: 3 full days of withdrawal; protein levels: intoxicated) were used for each set of experiments. Regarding this latter point, it is important to note that elevated glutamatergic transmission was observed at both time points, while the decreases in protein and gene expression were measured during intoxication and at 3-days withdrawal, respectively. We chose to focus our AMPAR-mediated neurotransmission recordings on layer 2/3 pyramidal neurons of the prelimbic

mPFC as we have found this layer/subregion to be particularly sensitive to chronic ethanol [33,40]. In the present study we found that dependence enhanced AMPAR function (similar to [33,39]), but it was recently reported that binge ethanol drinking reduced glutamate release onto prelimbic mPFC layer 2/3 pyramidal neurons of male and female mice, with no change in postsynaptic glutamate receptor function [12]. Given the more moderate and shorter drinking-in-the-dark model used by Crowley et al., we speculate that while ethanol may initially act on glutamatergic inputs, the heavier and longer ethanol exposure in our CIE-2BC model produces more enduring postsynaptic glutamate receptor adaptations (though see [21]). In support, we and others have found that several weeks of chronic intermittent ethanol vapor exposure generated widespread structural reorganization of prelimbic mPFC layer 2/3 pyramidal neurons by increasing their dendritic arborization, spine density and spine maturation [16,18,33].

In contrast to our functional work, our gene and protein expression studies were performed on mPFC tissue punches; therefore, the molecular changes that underlie our electrophysiology findings might have been diluted or masked by ethanol's effects on other mPFC subregions, layers, and cell types. Overall, we found that dependence/withdrawal decreased mPFC *Gria1/GluA1* and *Gria2* levels, suggesting that the chronic ethanol exposure itself may be the initial trigger for AMPAR plasticity though the withdrawal period could also independently contribute. Other studies have observed mixed effects of chronic ethanol and withdrawal on PFC/mPFC AMPAR expression, though no other studies to our knowledge have examined both timepoints. Specifically, chronic ethanol increased GluA1–3 in cortical neuronal culture [48] and in the PFC of binge-drinking mice withdrawn for 3 weeks [49], but had no effect on *GRIA1* and *GRIA2* mRNA in the dorsolateral PFC of heavy-drinking male cynomolgus monkeys [27] or on mPFC GluA1 in CIE-exposed mice withdrawn for one week [20]. There were also no differences in AMPAR subunit mRNA levels in *postmortem* dorsolateral PFC tissue from individuals with AUD compared with controls [50], though another study using *postmortem* PFC tissue from individuals with AUD identified *GRIA1* as a hub gene [32]. Finally, we assessed the phosphorylation ratio of GluA1-Ser831, since it can enhance AMPAR conductance [34], but found no change with dependence. Together with these mixed findings, our data suggest that the glutamate dysfunction caused by dependence may not be directly mediated by AMPAR expression or subunit composition.

Another mechanism of glutamatergic plasticity we explored is AMPAR synaptic targeting, which is when AMPARs are trafficked to extrasynaptic sites and then laterally diffuse into the synapse where they are captured by the synaptic scaffolding protein PSD95 [26]. Of note, GluA1-Ser845 phosphorylation mediates extrasynaptic AMPAR trafficking [35], while GRIP1 bidirectionally regulates the trafficking and synaptic targeting of GluA2/3-containing AMPARs [26]. Surprisingly, we found no change in GluA1-Ser845 phosphorylation ratio and decreased *Dlg4* and *Grip1* gene expression after chronic ethanol, but there are several other plasticity proteins implicated in ethanol's glutamatergic effects. For example, intrabasolateral amygdalar pharmacological inhibition of transmembrane AMPAR regulatory protein γ -8 (TARP γ -8), which is an AMPAR auxiliary subunit involved in its trafficking and activity, decreased ethanol self-administration in mice [51].

One major limitation of our work is that all experiments used male mice, which limits the generalizability of our findings. Specifically, there are significant sex differences in the PFC/mPFC glutamate system related to its neurotransmission, receptors, and transporters, as well as its plasticity-related proteins (e.g. PSD95), with brain glutamate receptor levels fluctuating across estrous cycle [4,52]. Most relevant to the present study, female mice display enhanced glutamate release and postsynaptic glutamate receptor function in mPFC layer 5 pyramidal neurons, and also have higher mPFC synaptosomal GluA1 expression compared to male mice [52]. It is not known whether similar sex differences exist in prelimbic mPFC layer 2/3 pyramidal neurons, but future studies should consider sex as a biological variable.

Likewise, most preclinical work that has probed AMPARs as mediators of ethanol reinforcement, seeking, drinking and relapse behavior has only used males [4,53–59]. Global knockdown studies in male mice suggest that ethanol's behavioral effects may be dependent on specific AMPAR subunits (i.e. GluA3, but not GluA1), but they could also be attributed to compensatory changes in other subunits or an overall reduction in AMPAR-mediated neurotransmission [55,58]. While no studies have investigated the contribution of mPFC AMPARs to ethanol-induced behaviors, several other addiction-related brain regions have been examined. For example, chronic ethanol increased synaptic GluA1 and GluA2 in the dorsomedial striatum and pharmacological inhibition of these AMPARs decreased ethanol self-administration in male rats with a history of excessive ethanol consumption [59]. Similarly, AMPAR activity in the dorsolateral striatum mediates binge-like ethanol drinking in male and female mice, though no concurrent changes in GluA1 or GluA2 expression were observed [53]. Finally, studies have identified a role for GluA1-containing AMPARs in the lateral habenula, basolateral amygdala and central amygdala in ethanol consumption and self-administration, with Ca²⁺/calmodulin-dependent protein kinase II (CaMKII)-mediated phosphorylation of GluA1-Ser831 also implicated [54,56,57,60]. Since pharmacological blockade of mPFC CaMKII in male mice increased the positive reinforcing effects of ethanol, this suggests that mPFC AMPAR signaling may uniquely inhibit ethanol-related behaviors [61]. mPFC AMPAR synaptic targeting and function also govern cognitive function [26], and so future studies should directly assess the role of mPFC AMPARs in ethanol consumption and associated cognitive deficits.

Collectively, these data highlight a role for mPFC AMPAR plasticity in the glutamatergic dysfunction associated with ethanol withdrawal. Given the importance of AMPAR in mediating most PFC fast excitatory synaptic transmission, directly targeting its function to treat AUD is less feasible [5,26]. However, future studies on the underlying AMPAR plasticity mechanisms that promote alcohol reinforcement, seeking, drinking and relapse behavior may help identify new targets for AUD treatment.

Supplementary Material

Refer to Web version on PubMed Central for supplementary material.

Acknowledgements

This is manuscript number 30247 from The Scripps Research Institute. This work was supported by the National Institutes of Health [AA025408 (FPV), AA017823 (FPV), AA031101 (FPV), AA013498 (MR), AA027700 (MR), AA021491 (MR), AA017447 (MR), AA006420 (MR, AJR, CC), AA029841 (MR), AA026685 (CC), AA027636 (CC), and AA025996 (SE)]; the Pearson Center for Alcoholism and Addiction Research; the TSRI Animal Models Core Facility; and The Schimmel Family Chair. The authors declare no competing financial interests, and the funding sources had no role in study design; in the collection, analysis and interpretation of data; in the writing of the report; and in the decision to submit the article for publication.

Data availability

Data will be made available on request.

Abbreviations:

aCSF	artificial cerebrospinal fluid
AMPAR	α -amino-3-hydroxy-5-methyl-4-isoxazolepropionic acid-type ionotropic glutamate receptor
AUD	alcohol use disorder
BEL	blood ethanol level
CAMKII	calcium/calmodulin-dependent protein kinase II
CIE	chronic intermittent ethanol vapor model
CIE-2BC	chronic intermittent ethanol vapor-two bottle choice model
Dep	ethanol dependent mice
DLG4	discs large MAGUK scaffold protein 4
<i>Gria1-4</i>	glutamate ionotropic receptor AMPA type subunit 1-4
<i>Grip1</i>	glutamate receptor interacting protein 1
LTD	long-term depression
LTP	long-term potentiation
mPFC	medial prefrontal cortex
mEPSC	miniature excitatory postsynaptic current
NMDAR	N-methyl-D-aspartate receptor
Non-dep	non-dependent mice
PSD95	postsynaptic density protein 95
rt-PCR	real time polymerase chain reaction
sEPSC	spontaneous excitatory postsynaptic current

2BC	two bottle choice ethanol drinking
<i>Tbp</i>	TATA-binding protein

References

- [1]. Zahr NM, et al. , Perspectives on fronto-fugal circuitry from human imaging of alcohol use disorders, *Neuropharmacology* 122 (2017) 189–200. [PubMed: 28118989]
- [2]. Hu Y, et al. , Glutamate levels in the ventromedial prefrontal cortex and resting-state functional connectivity within reward circuits in alcohol-dependent patients, *Addict. Biol* 28 (2023) e13272. [PubMed: 37016753]
- [3]. Gass JT, Olive MF, Glutamatergic substrates of drug addiction and alcoholism, *Biochem. Pharmacol* 75 (2008) 218–265. [PubMed: 17706608]
- [4]. Giacometti LL, Barker JM, Sex differences in the glutamate system: implications for addiction, *Neurosci. Biobehav. Rev* 113 (2020) 157–168. [PubMed: 32173404]
- [5]. Kalivas PW, Volkow ND, New medications for drug addiction hiding in glutamatergic neuroplasticity, *Mol. Psychiatry* 16 (2011) 974–986. [PubMed: 21519339]
- [6]. Bauer J, et al. , Craving in alcohol-dependent patients after detoxification is related to glutamatergic dysfunction in the nucleus accumbens and the anterior cingulate cortex, *Neuropsychopharmacology* 38 (2013) 1401–1408. [PubMed: 23403696]
- [7]. Frye MA, et al. , Elevated glutamate levels in the left dorsolateral prefrontal cortex are associated with higher cravings for alcohol, *Alcohol Clin. Exp. Res* 40 (2016) 1609–1616. [PubMed: 27439218]
- [8]. Hermann D, et al. , Translational magnetic resonance spectroscopy reveals excessive central glutamate levels during alcohol withdrawal in humans and rats, *Biol. Psychiatry* 71 (2012) 1015–1021. [PubMed: 21907974]
- [9]. Ende G, et al. , Loss of control of alcohol use and severity of alcohol dependence in non-treatment-seeking heavy drinkers are related to lower glutamate in frontal white matter, *Alcohol Clin. Exp. Res* 37 (2013) 1643–1649. [PubMed: 23800328]
- [10]. Mon A, et al. , Glutamate, GABA, and other cortical metabolite concentrations during early abstinence from alcohol and their associations with neurocognitive changes, *Drug Alcohol Depend.* 125 (2012) 27–36. [PubMed: 22503310]
- [11]. Yeo RA, et al. , Neurometabolite concentration and clinical features of chronic alcohol use: a proton magnetic resonance spectroscopy study, *Psychiatry Res.* 211 (2013) 141–147. [PubMed: 23154093]
- [12]. Crowley NA, et al. , Ketamine normalizes binge drinking-induced defects in glutamatergic synaptic transmission and ethanol drinking behavior in female but not male mice, *Neuropharmacology* 149 (2019) 35–44. [PubMed: 30731135]
- [13]. Galaj E, et al. , Contrasting effects of adolescent and early-adult ethanol exposure on prelimbic cortical pyramidal neurons, *Drug Alcohol Depend.* 216 (2020), 108309. [PubMed: 32998090]
- [14]. Gass JT, et al. , Enhancement of extinction learning attenuates ethanol-seeking behavior and alters plasticity in the prefrontal cortex, *J. Neurosci* 34 (2014) 7562–7574. [PubMed: 24872560]
- [15]. George O, et al. , Recruitment of medial prefrontal cortex neurons during alcohol withdrawal predicts cognitive impairment and excessive alcohol drinking, *Proc. Natl. Acad. Sci. USA* 109 (2012) 18156–18161. [PubMed: 23071333]
- [16]. Holmes A, et al. , Chronic alcohol remodels prefrontal neurons and disrupts NMDAR-mediated fear extinction encoding, *Nat. Neurosci* 15 (2012) 1359–1361. [PubMed: 22941108]
- [17]. Joffe ME, et al. , Increased synaptic strength and mGlu2/3 receptor plasticity on mouse prefrontal cortex intra-telencephalic pyramidal cells following intermittent access to ethanol, *Alcohol Clin. Exp. Res* 45 (2021) 518–529. [PubMed: 33434325]
- [18]. Kim A, et al. , Structural reorganization of pyramidal neurons in the medial prefrontal cortex of alcohol dependent rats is associated with altered glial plasticity, *Brain Struct. Funct* 220 (2015) 1705–1720. [PubMed: 24667898]

- [19]. Klenowski PM, et al. , Increased synaptic excitation and abnormal dendritic structure of prefrontal cortex layer V pyramidal neurons following prolonged binge-like consumption of ethanol, *eNeuro* 3 (2016). ENEURO.0248-16.2016.
- [20]. Kroener S, et al. , Chronic alcohol exposure alters behavioral and synaptic plasticity of the rodent prefrontal cortex, *PLoS One* 7 (2012) e37541. [PubMed: 22666364]
- [21]. Pleil KE, et al. , Effects of chronic ethanol exposure on neuronal function in the prefrontal cortex and extended amygdala, *Neuropharmacology* 99 (2015) 735–749. [PubMed: 26188147]
- [22]. Smith RJ, et al. , Dynamic c-Fos changes in mouse brain during acute and protracted withdrawal from chronic intermittent ethanol exposure and relapse drinking, *Addict. Biol* 25 (2020) e12804. [PubMed: 31288295]
- [23]. Trantham-Davidson H, et al. , Chronic alcohol disrupts dopamine receptor activity and the cognitive function of the medial prefrontal cortex, *J. Neurosci* 34 (2014) 3706–3718. [PubMed: 24599469]
- [24]. Roberto M, Varodayan F, Synaptic targets: chronic alcohol actions, *Neuropharmacology* 122 (2017) 85–99. [PubMed: 28108359]
- [25]. Weitlauf C, Woodward JJ, Ethanol selectively attenuates NMDAR-mediated synaptic transmission in the prefrontal cortex, *Alcohol Clin. Exp. Res* 32 (2008) 690–698. [PubMed: 18341645]
- [26]. Henley JM, Wilkinson KA, Synaptic AMPA receptor composition in development, plasticity and disease, *Nat. Rev. Neurosci* 17 (2016) 337–350. [PubMed: 27080385]
- [27]. Acosta G, et al. , Alternative splicing of AMPA subunits in prefrontal cortical fields of cynomolgus monkeys following chronic ethanol self-administration, *Front Psychiatry* 2 (2011) 72. [PubMed: 22291662]
- [28]. Breese CR, et al. , Glutamate receptor subtype expression in human postmortem brain tissue from schizophrenics and alcohol abusers, *Brain Res.* 674 (1995) 82–90. [PubMed: 7773698]
- [29]. Freund G, Anderson KJ, Glutamate receptors in the frontal cortex of alcoholics, *Alcohol Clin. Exp. Res* 20 (1996) 1165–1172. [PubMed: 8904965]
- [30]. Kärkkäinen O, et al. , AMPA receptors in post-mortem brains of Cloninger type 1 and 2 alcoholics: a whole-hemisphere autoradiography study, *Psychiatry Res.* 214 (2013) 429–434. [PubMed: 24119876]
- [31]. Pickering C, et al. , Identification of neurotransmitter receptor genes involved in alcohol self-administration in the rat prefrontal cortex, hippocampus and amygdala, *Prog. Neuropsychopharmacol. Biol. Psychiatry* 31 (2007) 53–64. [PubMed: 16876304]
- [32]. Farris SP, Mayfield RD, RNA-Seq reveals novel transcriptional reorganization in human alcoholic brain, *Int. Rev. Neurobiol* 116 (2014) 275–300. [PubMed: 25172479]
- [33]. Varodayan FP, et al. , Morphological and functional evidence of increased excitatory signaling in the prelimbic cortex during ethanol withdrawal, *Neuropharmacology* 133 (2018) 470–480. [PubMed: 29471053]
- [34]. Jenkins MA, Traynelis SF, PKC phosphorylates GluA1-Ser831 to enhance AMPA receptor conductance, *Channels (Austin)* 6 (2012) 60–64. [PubMed: 22373567]
- [35]. Oh MC, et al. , Extrasynaptic membrane trafficking regulated by GluR1 serine 845 phosphorylation primes AMPA receptors for long-term potentiation, *J. Biol. Chem* 281 (2006) 752–758. [PubMed: 16272153]
- [36]. Athanason AC, et al. , Chronic ethanol alters adrenergic receptor gene expression and produces cognitive deficits in male mice, *Neurobiol. Stress* 24 (2023), 100542. [PubMed: 37197395]
- [37]. Becker HC, Lopez MF, Increased ethanol drinking after repeated chronic ethanol exposure and withdrawal experience in C57BL/6 mice, *Alcohol Clin. Exp. Res* 28 (2004) 1829–1838. [PubMed: 15608599]
- [38]. Huitron-Resendiz S, et al. , Effects of withdrawal from chronic intermittent ethanol exposure on sleep characteristics of female and male mice, *Alcohol Clin. Exp. Res* 42 (2018) 540–550. [PubMed: 29265376]
- [39]. Patel RR, et al. , Ethanol withdrawal-induced adaptations in prefrontal corticotropin releasing factor receptor 1-expressing neurons regulate anxiety and conditioned rewarding effects of ethanol, *Mol. Psychiatry* (2022), 10.1038/S41380-022-01642-3.

- [40]. Varodayan FP, et al. , Chronic ethanol induces a pro-inflammatory switch in interleukin-1 β regulation of GABAergic signaling in the medial prefrontal cortex of male mice, *Brain Behav. Immun* 110 (2023) 125–139. [PubMed: 36863493]
- [41]. Patel RR, et al. , IL-10 normalizes aberrant amygdala GABA transmission and reverses anxiety-like behavior and dependence-induced escalation of alcohol intake, *Prog. Neurobiol* 199 (2021), 101952. [PubMed: 33197496]
- [42]. Patel RR, et al. , IL-1 β expression is increased and regulates GABA transmission following chronic ethanol in mouse central amygdala, *Brain Behav. Immun* 75 (2019) 208–219. [PubMed: 30791967]
- [43]. Warden AS, et al. , Microglia control escalation of drinking in alcohol-dependent mice: genomic and synaptic drivers, *Biol. Psychiatry* 88 (2020) 910–921. [PubMed: 32680583]
- [44]. Sailing MC, Harrison NL, Strychnine-sensitive glycine receptors on pyramidal neurons in layers II/III of the mouse prefrontal cortex are tonically activated, *J. Neurophysiol* 112 (2014) 1169–1178. [PubMed: 24872538]
- [45]. Otis TS, et al. , Lasting potentiation of inhibition is associated with an increased number of gamma-aminobutyric acid type A receptors activated during miniature inhibitory postsynaptic currents, *Proc. Natl. Acad. Sci. USA* 91 (1994) 7698–7702. [PubMed: 8052645]
- [46]. Pahng AR, et al. , Neurobiological correlates of pain avoidance-like behavior in morphine-dependent and non-dependent rats, *Neuroscience* 366 (2017) 1–14. [PubMed: 29024786]
- [47]. Franklin K and Paxinos G (2008) *The mouse brain in stereotaxic coordinates, The Coronal Plates and Diagrams Compact, 3rd Edition.*
- [48]. Chandler LJ, et al. , Chronic ethanol upregulates NMDA and AMPA, but not kainate receptor subunit proteins in rat primary cortical cultures, *Alcohol.: Clin. Exper. Res* 23 (1999) 363–370. [PubMed: 10069569]
- [49]. Szumlinski KK, et al. , Alcohol-drinking during later life by C57BL/6 J mice induces sex- and age-dependent changes in hippocampal and prefrontal cortex expression of glutamate receptors and neuropathology markers, *Addict. Neurosci* 7 (2023), 100099. [PubMed: 37396410]
- [50]. Jin Z, et al. , Selective increases of AMPA, NMDA, and kainate receptor subunit mRNAs in the hippocampus and orbitofrontal cortex but not in prefrontal cortex of human alcoholics, *Front. Cell Neurosci* 8 (2014) 11. [PubMed: 24523671]
- [51]. Hoffman JL, et al. , Inhibition of AMPA receptors (AMPA) containing transmembrane AMPAR regulatory protein γ -8 with JNJ-55511118 shows preclinical efficacy in reducing chronic repetitive alcohol self-administration, *Alcohol Clin. Exp. Res* 45 (2021) 1424–1435. [PubMed: 34086361]
- [52]. Knouse MC, et al. , Sex differences in the medial prefrontal cortical glutamate system, *Biol. Sex Differ* 13 (2022) 66. [PubMed: 36348414]
- [53]. Bauer MR, et al. , Intra-dorsolateral striatal AMPA receptor antagonism reduces binge-like alcohol drinking in male and female C57BL/6 J mice, *Behav. Brain Res* 418 (2022), 113631. [PubMed: 34715146]
- [54]. Cannady R, et al. , Potentiation of amygdala AMPA receptor activity selectively promotes escalated alcohol self-administration in a CaMKII-dependent manner, *Addict. Biol* 22 (2017) 652–664. [PubMed: 26742808]
- [55]. Cowen MS, et al. , Neurobehavioral effects of alcohol in AMPA receptor subunit (GluR1) deficient mice, *Neuropharmacology* 45 (2003) 325–333. [PubMed: 12871650]
- [56]. Faccidomo S, et al. , Calcium-permeable AMPA receptor activity and GluA1 trafficking in the basolateral amygdala regulate operant alcohol self-administration, *Addict. Biol* 26 (2021) e13049. [PubMed: 33955100]
- [57]. Li J, et al. , Inhibition of AMPA receptor and CaMKII activity in the lateral habenula reduces depressive-like behavior and alcohol intake in rats, *Neuropharmacology* 126 (2017) 108–120. [PubMed: 28865912]
- [58]. Sanchis-Segura C, et al. , Involvement of the AMPA receptor GluR-C subunit in alcohol-seeking behavior and relapse, *J. Neurosci* 26 (2006) 1231–1238. [PubMed: 16436610]

- [59]. Wang J, et al. , Ethanol-mediated facilitation of AMPA receptor function in the dorsomedial striatum: implications for alcohol drinking behavior, *J. Neurosci* 32 (2012) 15124–15132. [PubMed: 23100433]
- [60]. Salling MC, et al. , Moderate alcohol drinking and the amygdala proteome: identification and validation of calcium/calmodulin dependent kinase II and AMPA receptor activity as novel molecular mechanisms of the positive reinforcing effects of alcohol, *Biol. Psychiatry* 79 (2016) 430–442. [PubMed: 25579851]
- [61]. Faccidomo S, et al. , CaMKII inhibition in the prefrontal cortex specifically increases the positive reinforcing effects of sweetened alcohol in C57BL/6 J mice, *Behav. Brain Res* 298 (2016) 286–290. [PubMed: 26608538]

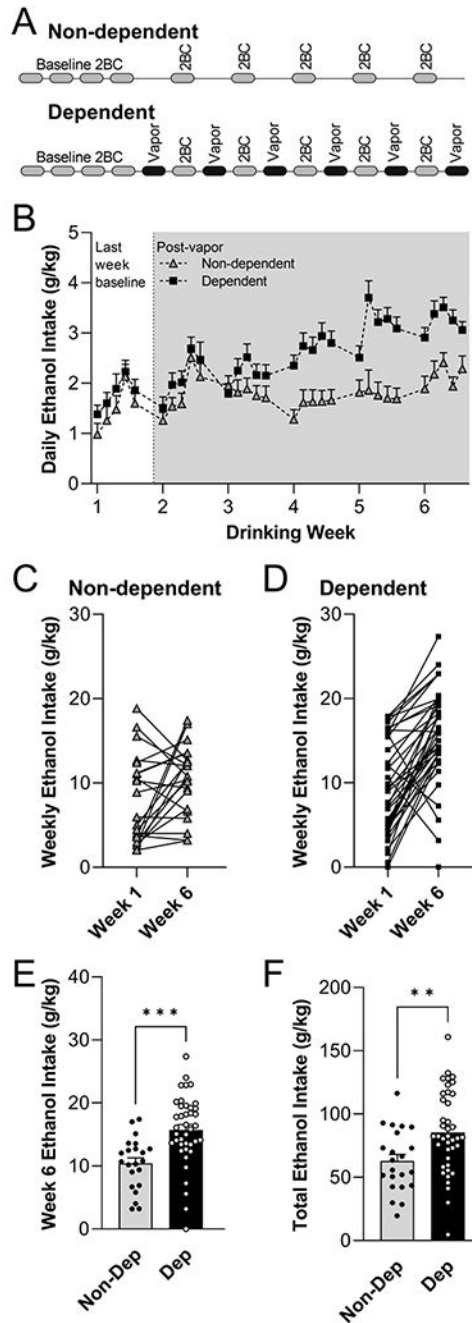


Fig. 1. Ethanol intake escalated in Dependent mice. **A.** Schematic of the CIE-2BC protocol used to generate ethanol dependence, with mice experiencing alternating weeks of chronic intermittent ethanol vapor (CIE) and two bottle choice ethanol drinking (2BC). Non-dependent mice experienced 2BC but not CIE. Naïve mice did not receive any ethanol exposure (not illustrated). **B.** There was an escalation of ethanol intake in the 2BC drinking sessions during Weeks 4–6 in the Dependent vs. Non-dependent mice. **C-D.** (C) 13 out of 22 Non-dependent mice increased their weekly ethanol intake from their last baseline week

to their final drinking week (Week 1 to Week 6), (D) while the majority of Dependent mice escalated their ethanol drinking during this time period (35/40 mice). E-F. Dependent mice had a higher ethanol intake (E) during the last week of 2BC (Week 6), and (F) totaled across all 2BC sessions vs. the Non-dependent group. $N = 22-40$ mice per group. ** $p < 0.01$, *** $p < 0.001$ by unpaired t -test.

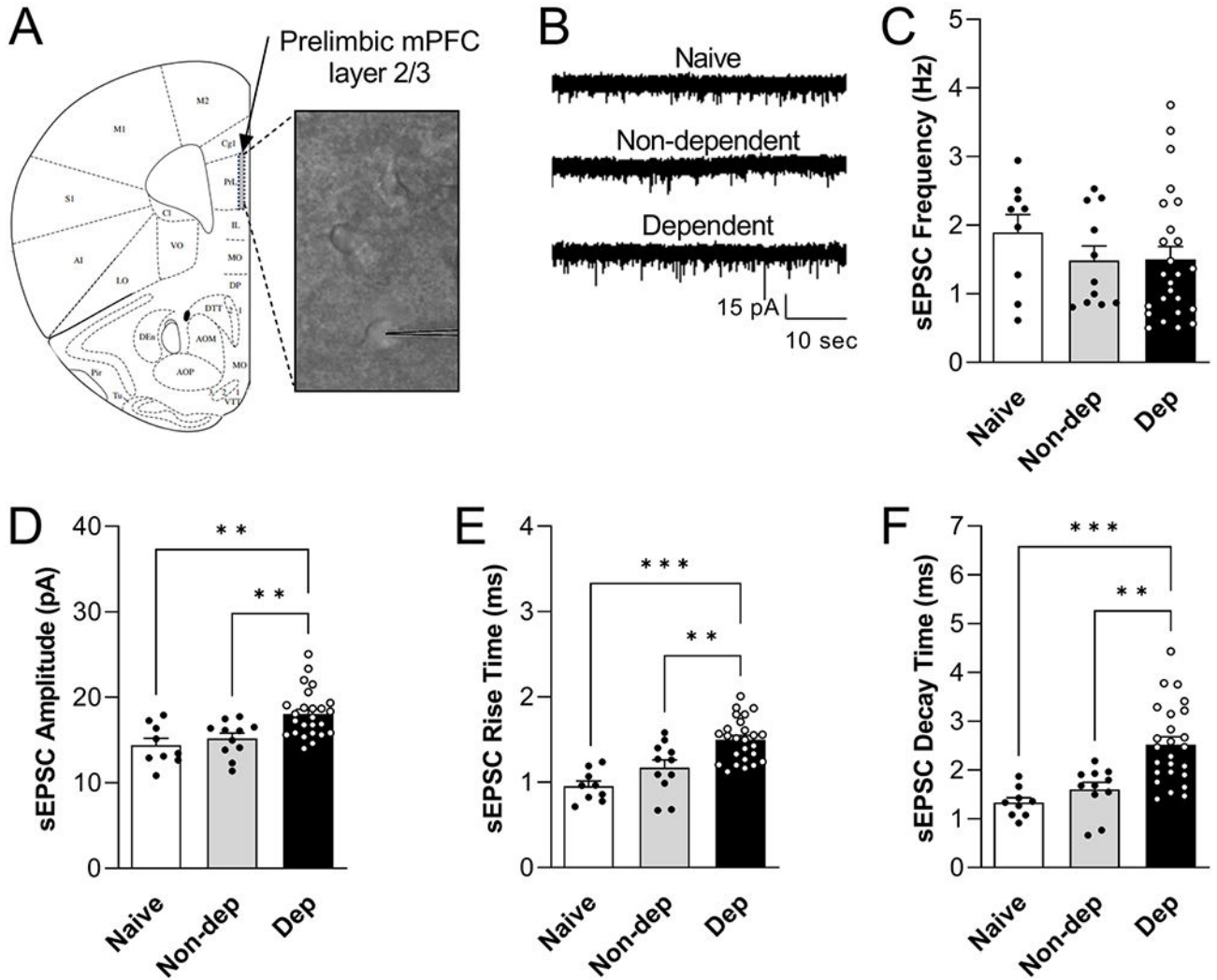


Fig. 2.

Ethanol dependence increased glutamate receptor function after 3–8 days withdrawal. A. Schematic of a coronal brain slice illustrating layer 2/3 of the prelimbic mPFC (adapted from [47]), and a 40x micrograph of a representative pyramidal neuron. B. Representative sEPSC traces from Naïve, Non-dependent and Dependent neurons. C. There was no significant difference in sEPSC frequency across mice groups. D–F. The sEPSC (D) amplitude, (E) rise time and (F) decay time were higher in Dependent vs. Naïve and Non-dependent mice, $n = 9–25$ cells from $N = 7–11$ mice per group. $**p < 0.01$; $***p < 0.001$ by one-way ANOVA and Tukey's *post hoc* test.

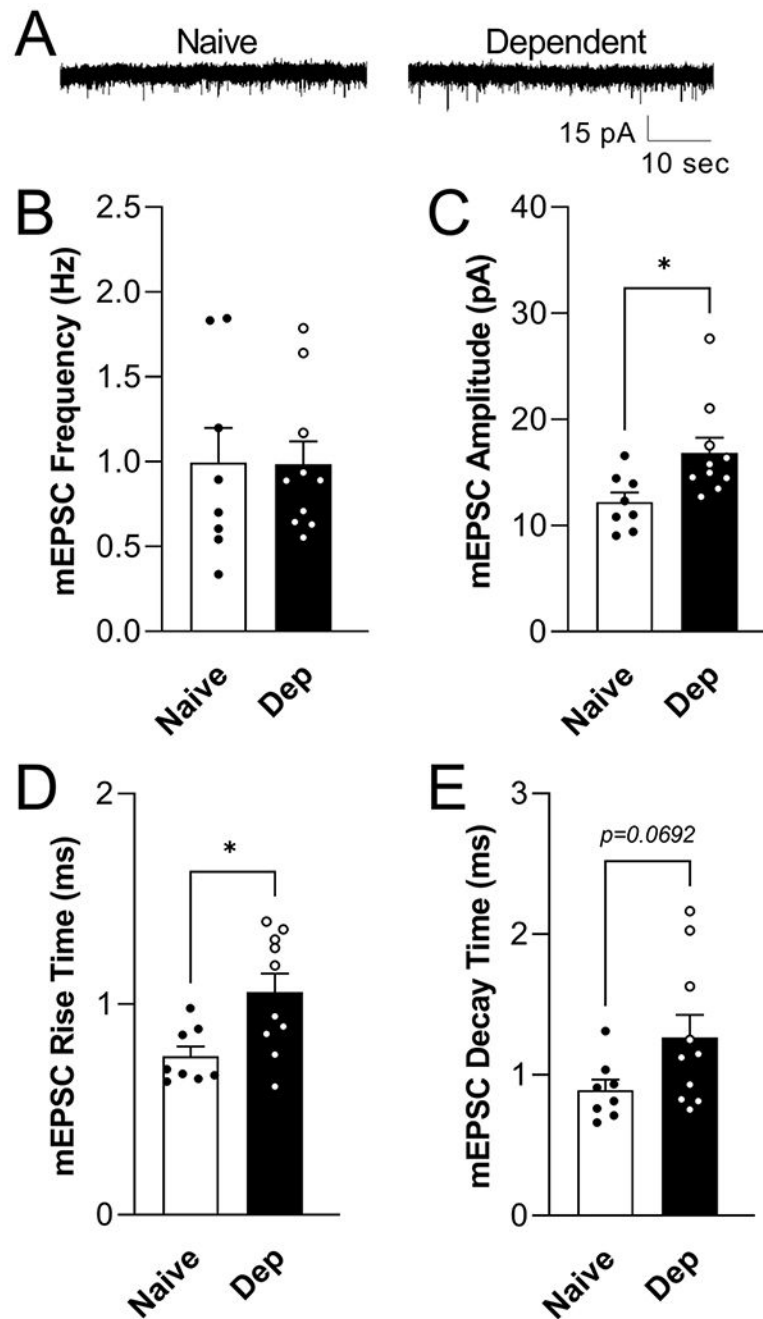
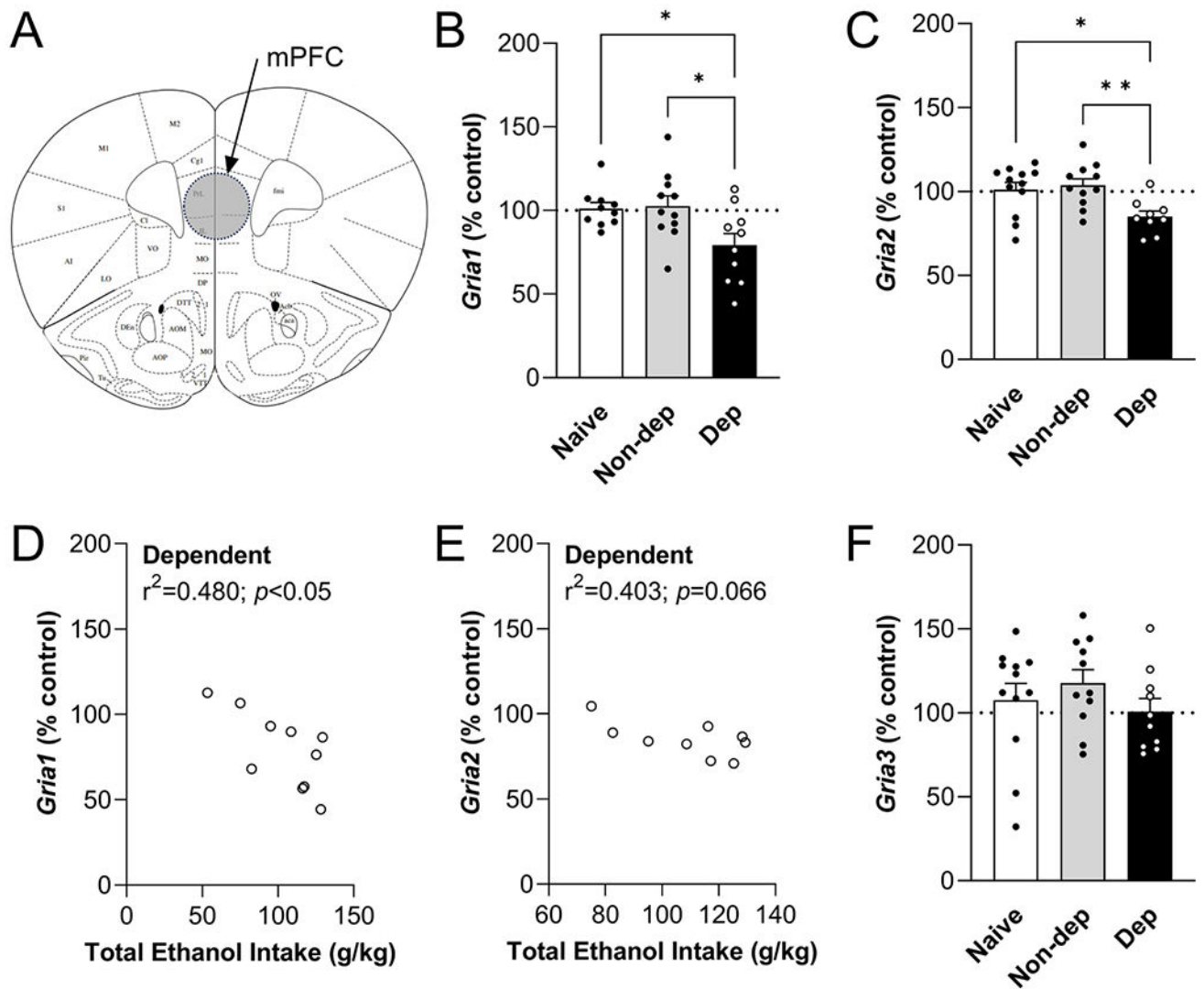


Fig. 3. Ethanol dependence increased glutamate receptor function via an action potential-independent mechanism. A. Representative mEPSC traces from Naïve and Dependent neurons. B. There was no significant difference in mEPSC frequency of mPFC prelimbic layer 2/3 pyramidal neurons between mice groups. C–E. The mEPSC (C) amplitude and (D) rise time were higher in Dependent vs. Naïve mice, while there was a trend approaching significance in the (E) decay time, $n = 8–12$ cells from $N = 5–6$ mice per group. * $p < 0.05$ by unpaired t -test.

**Fig. 4.**

Ethanol dependence decreased mPFC AMPAR subunit gene expression. A. Schematic of a coronal brain slice illustrating the mPFC micropunch site (adapted from [47]). B and C. Gene expression levels for (B) *Gria1* and (C) *Gria2* were lower in Dependent vs. Naïve and Non-dependent mice. D and E. Total ethanol intake within the Dependent group (D) negatively correlated with *Gria1* transcript levels, while there was a trend for a negative correlation in (E) *Gria2*. F. There was no difference in *Gria3* mRNA levels across all three mice groups. $N=9-12$ mice per group. * $p < 0.05$; ** $p < 0.01$ by one-way ANOVA and Tukey's *post hoc* test.

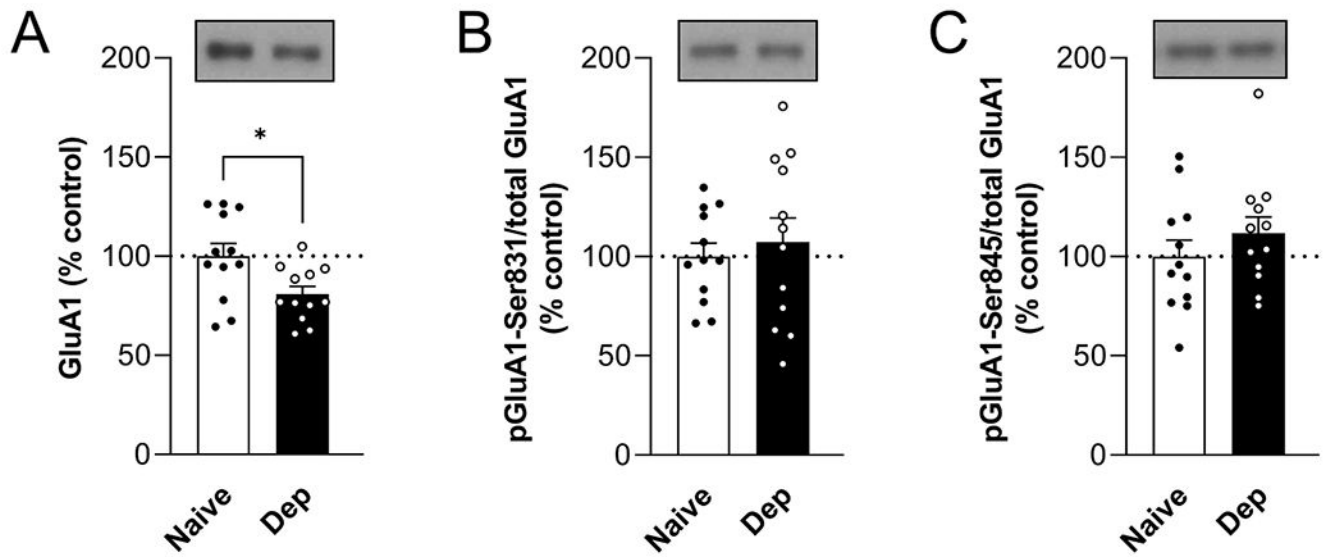


Fig. 5. Ethanol dependence decreased mPFC AMPAR subunit protein expression. A. GluA1 levels were lower in Dependent vs. Naïve mice. B and C. There was no difference in the phosphorylation ratios of (B) GluA1-Ser831 and (C) GluA1-Ser841 across both mice groups. $N=12$ mice per group. $*p < 0.05$ by unpaired t -test.

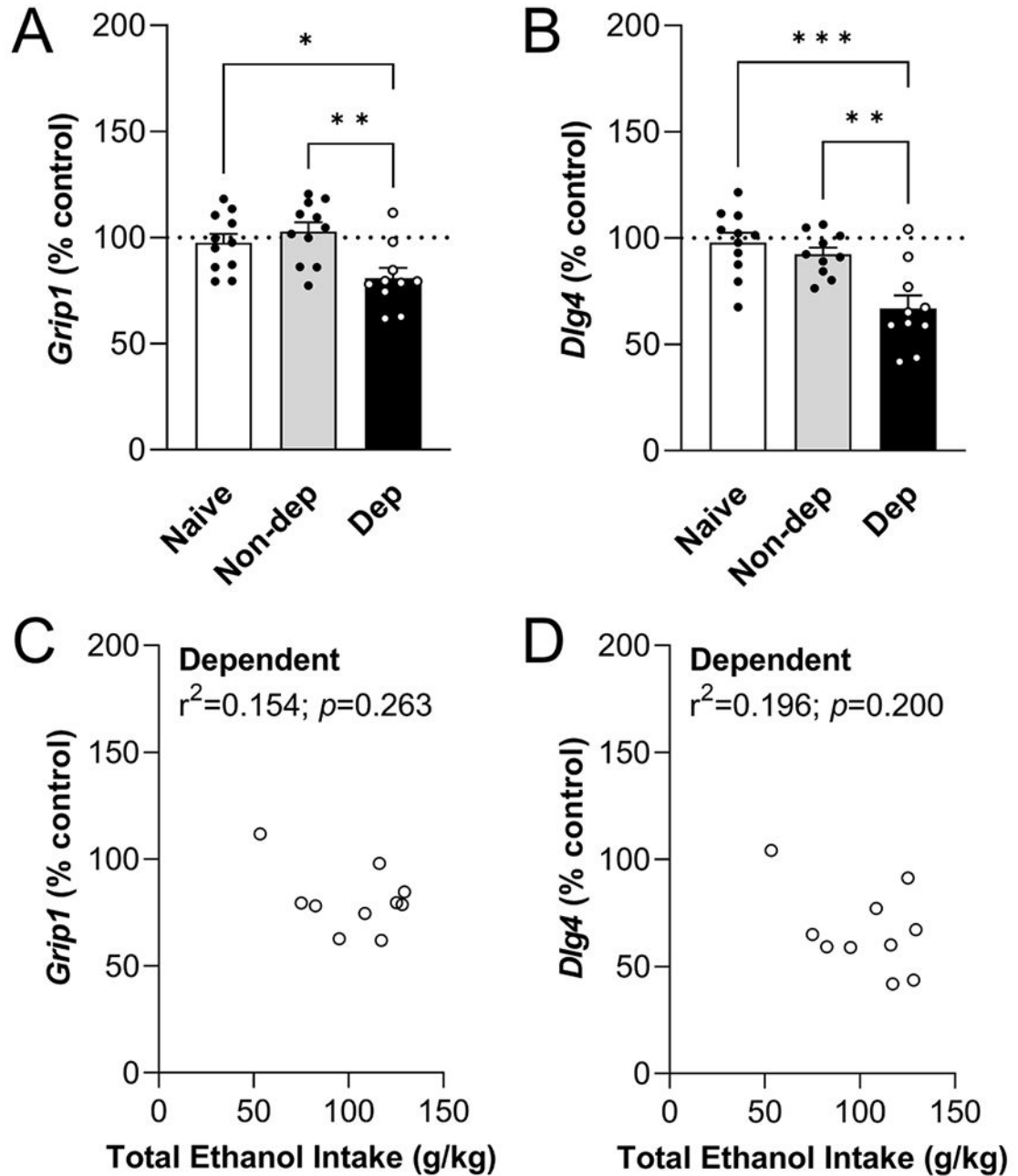


Fig. 6. Ethanol dependence decreased mPFC plasticity gene expression. A and B. mPFC mRNA levels for (A) *Grip1* and (B) *Dlg4* were lower in Dependent vs. Naïve and Non-dependent mice. C and D. There were no significant correlations between the total ethanol intake of the Dependent group and (C) *Grip1* and (D) *Dlg4* transcript levels. $N= 10-11$ mice per group. * $p < 0.05$; ** $p < 0.01$; *** $p < 0.001$ by one-way ANOVA and Tukey's *post hoc* test.

Table 1

Details about primer pairs used for the gene expression study.

Gene name	Gene symbol	Accession number	Forward primer	Reverse primer
TATA-box binding protein	<i>Thp</i>	NM_013684.3	TTCTGCGGTCGCGTCATT	GTGGAAGGCTGTGTGTTCTGGT
Glutamate ionotropic receptor AMPA type subunit 1	<i>Gria1</i>	NM_008165.4, NM_001113325.2, NM_001252403.1	TGGAAGCCGGATGAAGGGTTT	GGATTGCATGGACTTTGGGGA
Glutamate ionotropic receptor AMPA type subunit 2	<i>Gria2</i>	NM_013540.4, NM_001039195.3, NM_001083806.3, NM_001357924.2, NM_001357927.2	GCGTGTAATCCTTTGACTGCG	GGTCTCCATCAGTAAATCCCAGA
Glutamate ionotropic receptor AMPA type subunit 3	<i>Gria3</i>	NM_016886.5, NM_001281929.2, NM_001290451.3, NM_001358361.2	CTTAGCAAATCCTGCTGTGCC	TCATTCCAGTAACCAAGCTTTTTCG
Glutamate receptor interacting protein 1	<i>Grip1</i>	NM_028736.2, NM_130,891.2, NM_133,442.2, NM_001277292.1, NM_001277293.1, NM_001277294.1, NM_001277295.1, NM_001358809.1, NM_001358810.1, NM_001358811.1	CCATCAGAGCAAAGTCACAC	TTTCTACTGGATGGCGAACTGA
Discs large MAGUK scaffold protein 4 (also known as postsynaptic density 95 or PSD95)	<i>Dlg4</i>	NM_007864.3, NM_001109752.1, NM_001370671.1, NM_001370672.1, NM_001370674.1, NM_001370675.1	GGCTTCATCCCAAGAAAACG	CCGAGTCTTCTCGACCCCTGT

Table 2

Statistical values for the gene expression study.

Gene symbol	Statistical value
<i>Tbp</i>	$F(2,30) = 1.85, p = 0.18$
<i>Gria1</i>	$F(2,28) = 4.92, p < 0.05$
<i>Gria2</i>	$F(2,29) = 5.78, p < 0.01$
<i>Gria3</i>	$F(2,29) = 1.24, p = 0.31$
<i>Grip1</i>	$F(2,29) = 6.67, p < 0.01$
<i>Dlg4</i>	$F(2,28) = 11.72, p < 0.001$

Author Manuscript

Author Manuscript

Author Manuscript

Author Manuscript